

A fast-reliable methodology to estimate the concentration of rutile or anatase phases of TiO₂

A. R. Zanatta

Citation: *AIP Advances* **7**, 075201 (2017); doi: 10.1063/1.4992130

View online: <http://dx.doi.org/10.1063/1.4992130>

View Table of Contents: <http://aip.scitation.org/toc/adv/7/7>

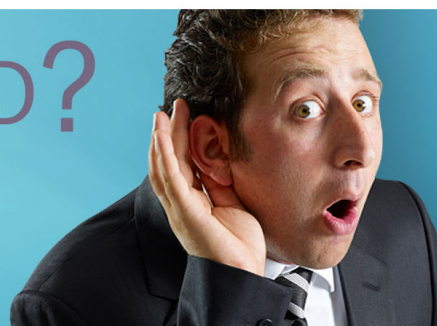
Published by the [American Institute of Physics](#)

HAVE YOU HEARD?

Employers hiring scientists and
engineers trust

PHYSICS TODAY | JOBS

www.physicstoday.org/jobs



A fast-reliable methodology to estimate the concentration of rutile or anatase phases of TiO₂

A. R. Zanatta^a

Instituto de Física de São Carlos, Universidade de São Paulo, São Carlos, SP 13560-590, Brazil

(Received 10 May 2017; accepted 26 June 2017; published online 5 July 2017)

Titanium-dioxide (TiO₂) is a low-cost, chemically inert material that became the basis of many modern applications ranging from, for example, cosmetics to photovoltaics. TiO₂ exists in three different crystal phases – Rutile, Anatase and, less commonly, Brookite – and, in most of the cases, the presence or relative amount of these phases are essential to decide the TiO₂ final application and its related efficiency. Traditionally, X-ray diffraction has been chosen to study TiO₂ and provides both the phases identification and the Rutile-to-Anatase ratio. Similar information can be achieved from Raman scattering spectroscopy that, additionally, is versatile and involves rather simple instrumentation. Motivated by these aspects this work took into account various TiO₂ Rutile+Anatase powder mixtures and their corresponding Raman spectra. Essentially, the method described here was based upon the fact that the Rutile and Anatase crystal phases have distinctive phonon features, and therefore, the composition of the TiO₂ mixtures can be readily assessed from their Raman spectra. The experimental results clearly demonstrate the suitability of Raman spectroscopy in estimating the concentration of Rutile or Anatase in TiO₂ and is expected to influence the study of TiO₂-related thin films, interfaces, systems with reduced dimensions, and devices like photocatalytic and solar cells. © 2017 Author(s). All article content, except where otherwise noted, is licensed under a Creative Commons Attribution (CC BY) license (<http://creativecommons.org/licenses/by/4.0/>). [<http://dx.doi.org/10.1063/1.4992130>]

I. INTRODUCTION

Titanium dioxide TiO₂, also known as titania, is a semiconductor material with applications in technological fields such as: photovoltaics,^{1,2} energy storage,³ photocatalysis⁴ – with emphasis on environmental⁵ and health problems,⁶ optical coatings⁷ and sensors,⁸ just to mention a few of them.

Rutile and Anatase are the two main polymorphs of TiO₂ in which the tetragonal coordination applies.⁹ The third polymorph of TiO₂ is Brookite that presents orthorhombic coordination and that is the unusual phase of TiO₂.¹⁰ Along with Anatase, Brookite is metastable and irreversibly transformed into Rutile over a range of temperatures.¹¹ In terms of their electronic properties, the optical bandgaps (E_g) of the TiO₂ polymorphs take place in the ultraviolet region ($E_g^{\text{Rut}} \sim 3.0$ eV (or ~ 413 nm), $E_g^{\text{Brook}} \sim 3.3$ eV (~ 375 nm), and $E_g^{\text{Anat}} \sim 3.4$ eV (~ 365 nm)¹²) suggesting the limited (or no) utility of natural TiO₂ in applications involving visible or solar radiation. In spite of this, the atomic structure and optical properties of TiO₂ can be adjusted to comply with the desired application, and the literature is plenty of successful examples of TiO₂ in photovoltaics¹³ and photocatalysis.¹⁴ In fact, the structural and optical properties of TiO₂ are crucial in determining not only the application target but, specially, its final performance. A classical demonstration of such influence is the effect that the Rutile-Anatase phases exert on the efficiency of TiO₂-based dye-sensitized solar cells (DSSC), amongst which one can mention: larger interfacial area provided by nanocrystalline Rutile to extract photogenerated electrons,¹⁵ electron energy shift from Rutile to Anatase to compensate variations

^azanatta@ifsc.usp.br

in the photoelectrodes area,¹⁶ and improved short-circuit current due to the higher light scattering originated from Rutile.¹⁷ Accordingly, the identification and quantification of the TiO₂ polymorphs is of great importance in the research and development of TiO₂-based materials and devices.

Along the years, X-ray diffraction (XRD) has been the preferred technique to study TiO₂, efficiently exposing the presence of the Rutile, Anatase, and Brookite phases, their crystal orientation, and the Rutile-to-Anatase ratio.¹¹ Raman scattering spectroscopy is also able to precisely distinguish between the different TiO₂ crystal phases but, so far, the technique presented certain restrictions to evaluate the Rutile or Anatase concentrations. Most of these shortcomings relied on:¹⁸⁻²² (i) the recurring interest in the very strong Anatase-related phonon mode at ~ 144 cm⁻¹ that, unfortunately, is also present in the Rutile phase; (ii) the study of a limited range of Rutile or Anatase concentrations precluding any reliable conclusion; and (iii) the lack of a simple relationship – connecting the Rutile or Anatase contents with their respective Raman features – that explains, at the same time, the whole range of concentrations.

These aspects define the purpose of the present work which shows the ability of Raman spectroscopy towards the quantitative determination of the Rutile or Anatase phases in TiO₂ powders. The study comprised several TiO₂ mixtures, containing different amounts of Rutile and Anatase, and their corresponding Raman spectra. The experimental results indicate a clear correlation between the Rutile concentrations and the Raman data, as provided by the analysis of the proper Rutile- and Anatase-related phonon modes. Within this context, Raman spectroscopy represents a powerful characterization technique – acting either identifying or computing the Rutile or Anatase phases of TiO₂ – that is expected to advance the research of TiO₂-containing materials with dimensions in the sub-micrometers range and/or in the form of thin films.

II. EXPERIMENTAL DETAILS

All samples considered in the present work were achieved from commercial TiO₂ powders by mixing different amounts of the Anatase and Rutile phases in a digital balance (mass precision 100 µg). The mixtures ranged from pure Anatase to pure Rutile and were identified according to the relative mass of Rutile as defined by:

$$M_{\text{Rut}} = \frac{\text{mass}_{\text{Rutile}}}{\text{mass}_{\text{Rutile}} + \text{mass}_{\text{Anatase}}}. \quad (1)$$

An experimental accuracy of about 2.5% was attributed to M_{Rut} which took into account the purity of the original Anatase and Rutile powders (> 99.99%), as well as eventual errors associated with the weighting, handling, and homogenization of the powder samples. The TiO₂ mixtures were investigated by X-ray diffraction (XRD) and Raman scattering spectroscopy. The XRD measurements employed the Cu K α radiation (1.5406 Å) and a Bragg-Brentano θ -2 θ configuration. The diffractograms were registered in the 20-60° range with a step size of 0.02° (slit width of 0.3 mm) and, typically, the x-ray beam probed a sample area of ~ 50 mm². The Raman spectra were obtained in the ~ 50-1500 cm⁻¹ spectral range by exciting the samples with a HeNe laser (632.8 nm) in the backscattering geometry. With the help of an optical microscope, Raman measurements can probe, selectively, sample areas as small as ~ 0.2 µm² (x100 objective lens). However, in the present study, a ~ 80 µm² (x5 objective lens) analyzed area and very low laser power (30 µW) were considered.

Following the above experimental conditions each XRD and Raman scan took around 30 and 6 min, respectively. These figures can be reduced by a factor of 4, with no loss of accuracy nor information, by limiting the scanned ranges just to the regions of interest: 20-30° and 100-1000 cm⁻¹, for example. All measurements were carried out at room atmosphere and temperature.

III. RESULTS AND DISCUSSION

Allied to its relative simplicity, the XRD technique is well-known by its high efficiency in determining the atomic structure-composition of materials.²³ That arises from the fact that: to each XRD peak (diffraction angle and diffraction intensity) corresponds a particular set of atomic planes (arrangement and amount). Hence, XRD is particularly useful to study TiO₂ since it clearly indicates the presence of the Anatase and Rutile phases and yields a good estimate of their concentrations.²⁴

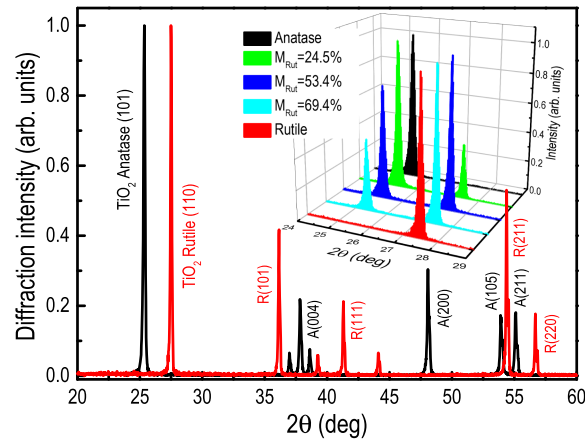


FIG. 1. XRD diffractograms of TiO_2 powders with only the pure Anatase ($M_{\text{Rut}} = 0\%$) or Rutile ($M_{\text{Rut}} = 100\%$) phases. The crystal orientation of some diffraction peaks are indicated in the figure. The inset presents the XRD pattern, in the $24\text{--}29^\circ$ diffraction range, of samples with different amounts of Rutile (M_{Rut}). All diffractograms were normalized for comparison purposes.

These aspects are illustrated in Figure 1, which shows the XRD pattern of TiO_2 powders containing either the pure Anatase ($M_{\text{Rut}} = 0\%$) or Rutile ($M_{\text{Rut}} = 100\%$) phases. The crystal orientation of some diffraction peaks were also indicated in the figure according to the JCPDS card files #21-1272 (A for Anatase) and #21-1276 (R for Rutile). Within the most prominent crystal features present in Fig. 1, are the A(101) and R(110) that occur at 25.36° and 27.49° , respectively. A closer view of these two diffraction peaks is shown in the inset of Fig. 1 and points out their peculiar behavior for samples with $M_{\text{Rut}} = 0, 24.5, 53.4, 69.4,$ and 100% .

The effect of different M_{Rut} onto the A(101) and R(110) diffraction peaks of some of the present TiO_2 R+A mixtures were investigated in detail and their main results are shown in Figure 2. The figure presents the effect of M_{Rut} onto the concentration of Rutile (%Rut) as calculated in terms of either the area or the intensity ratios of the A(101) and R(110) diffraction peaks:

$$\% \text{Rut}(\text{Int}) = \frac{\text{Int}_{\text{R}(110)}}{\text{Int}_{\text{R}(110)} + \text{Int}_{\text{A}(101)}} \quad \text{and} \quad \% \text{Rut}(\text{Area}) = \frac{\text{Area}_{\text{R}(110)}}{\text{Area}_{\text{R}(110)} + \text{Area}_{\text{A}(101)}}. \quad (2)$$

The figure also shows the %Rut as estimated from the Spurr and Myers (S&M) equation, as well as the original data of S&M when studying similar TiO_2 R+A mixtures.²⁴ Based on the results of Fig. 2 it is clear that: (a) as expected, there is a good agreement (within $< 5\%$) between the calculated %Rut and the M_{Rut} values – either involving the XRD intensity or area estimates; (b) the original data of S&M (exclusively based on the $\text{Int}_{\text{A}(101)}/\text{Int}_{\text{R}(110)}$ ratio) also matches (within $\sim 2\%$) the %Rut *versus* M_{Rut} representation; and (c) the use of the S&M equation to the present TiO_2 R+A mixtures indicates Rutile contents almost 10% higher for the M_{Rut} in the $\sim 20\text{--}60\%$ range. Considering the great similarity of the TiO_2 phases (involving their X-ray mass absorption coefficient, for example) and the very same XRD acquisition conditions, the results of Fig. 2 show the failure of the S&M equation in estimating the Rutile or Anatase phase concentration. In fact, the results provided by the XRD-S&M methodology are well-known to be inherently susceptible to factors¹¹ such as: preferred orientation, crystal morphology and grain size, residual strain, presence of impurities, etc. A very appropriate way to overcome these issues is achieved by means of Raman scattering spectroscopy.

Just like XRD, Raman spectroscopy represents a powerful technique towards the identification and study of the structural-compositional properties of materials. It is non-destructive, requires no sample preparation, and its modern instrumentation (involving special optics, lasers, and large-area photon detectors) allows the study of very small areas in short times.²⁵ Moreover, Raman spectrometers can be found in portable/low-consumption versions and the technique is naturally suited to study thin films and in-line processes. Owing to these attributes, Raman spectroscopy has been applied to study the present TiO_2 R+A mixtures.

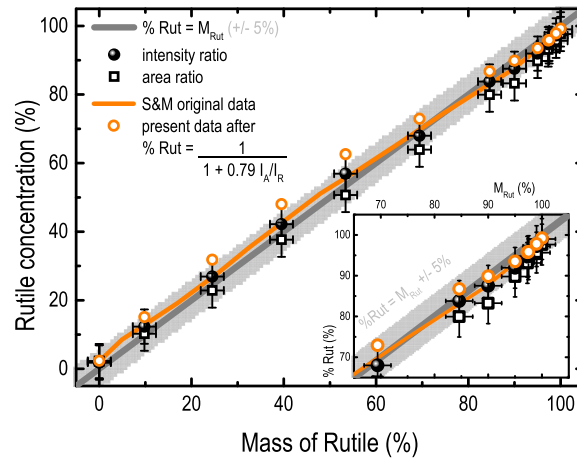


FIG. 2. Rutile concentration %Rut, as calculated from the intensity and the area ratios of the R(110) and A(101) x-ray diffraction data, as a function of the Rutile mass (M_{Rut}). The error bars took into consideration uncertainties in sample handling ($M_{\text{Rut}} \pm 2.5\%$) and data dispersion and processing ($\% \text{Rut} \pm 5\%$). Also shown in the figure are: a straight line denoting the linear relationship between the Rutile concentration and the mass of Rutile present in the mixture ($\% \text{Rut} = M_{\text{Rut}}$), the region in which $\% \text{Rut} = M_{\text{Rut}} \pm 5\%$, the original data of Spurr and Myers (S&M), and the Rutile concentration as determined by the S&M equation. The inset shows in detail the 65- 100% M_{Rut} range.

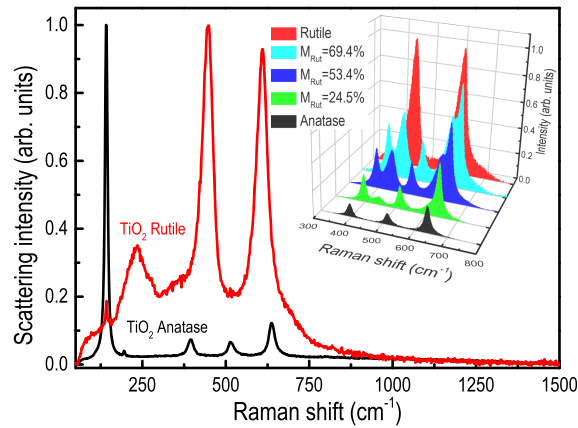


FIG. 3. Raman spectra of TiO_2 powders in the Anatase ($M_{\text{Rut}} = 0\%$) and Rutile ($M_{\text{Rut}} = 100\%$) phases. The inset illustrates the spectra of TiO_2 samples with different M_{Rut} values. In this case, the spectra were background corrected and intensity scaled for comparison purposes.

The Raman spectra of pure Anatase and Rutile are presented in Figure 3. According to the spectra, the frequency and symmetry assignment of the phonon modes due to the Rutile crystal phase take place at:²⁶ $143 \pm 1 \text{ cm}^{-1}$ (B_{1g}), $235 \pm 5 \text{ cm}^{-1}$ (combination of phonon modes), $448 \pm 2 \text{ cm}^{-1}$ (E_g), and $609 \pm 2 \text{ cm}^{-1}$ (A_{1g}). A weak mode (B_{2g}) is also verified at $826 \pm 5 \text{ cm}^{-1}$. Related to Anatase, the phonon modes appear at:²⁷ $144 \pm 1 \text{ cm}^{-1}$ (E_g), $196 \pm 1 \text{ cm}^{-1}$ (E_g), $395 \pm 1 \text{ cm}^{-1}$ (B_{1g}), $518 \pm 2 \text{ cm}^{-1}$ ($A_{1g} + B_{1g}$), and $639 \pm 1 \text{ cm}^{-1}$ (E_g). Extra (weak) peaks can be verified at 320 and 795 cm^{-1} and are related to the combination and to the overtone of other modes. In addition to these distinctive phonon modes it is worth to notice the high scattering intensity of Anatase at 144 cm^{-1} , as well as the presence of a broad ($\sim 50\text{-}800 \text{ cm}^{-1}$) background in the Rutile spectrum. The Raman spectra of some TiO_2 samples containing different M_{Rut} are shown in the inset of Fig. 3.

The spectra in the inset of Fig. 3 were shortened and had their background removed by a straight line from 300 to 800 cm^{-1} . Such spectral region and background removal procedure proved to be the most appropriate to evaluate the Rutile and Anatase phases present in the studied TiO_2 samples. Within the other approaches examined (*and their main drawbacks*) one can mention: (a) to consider all the Rutile and Anatase phonon modes in the $\sim 100\text{-}1000 \text{ cm}^{-1}$ spectral range (*high scattering intensity*

of the Anatase contribution at 144 cm^{-1}); (b) to consider all phonon modes combined with a broad *Gaussian*-like background (*high intensity of the Anatase mode at 144 cm^{-1} and Gaussian functions with very different parameters from sample to sample*); (c) the combination of different Rutile and Anatase phonon modes and their respective intensity or area ratios (*distinct regimes depending on M_{Rut}*); etc. In all of these cases, no single-reliable relationship involving M_{Rut} and the concentration of Rutile (or Anatase) was achieved.

In addition to the background removal in the $300\text{--}800\text{ cm}^{-1}$ range, the evaluation of the Rutile and Anatase phases by means of Raman spectroscopy included the fitting of individual phonon modes with either *Gaussian* or *Lorentzian* functions. The overall results yielded by any of these two mathematical functions were almost identical with R-squared values higher than (or equal) to 0.99. To perform such investigation, any data analysis software can be used. In the present study the OriginLab® platform²⁸ and the following criteria were applied to a total of five individual phonon modes (3Anat + 2Rut): (1) there exists no offset between them; (2) they were allowed to vary around their original frequencies (*i.e.*, those observed in pure Rutile or in pure Anatase) to within $\pm 5\text{ cm}^{-1}$; (3) their full width at half maximum (FWHM) were limited to 50 cm^{-1} – in close agreement with the values presented by the pure Rutile and Anatase phases; and (4) obviously, the area of each individual mode in the $300\text{ to }800\text{ cm}^{-1}$ range should be positive.

The results of the above method are illustrated in Figure 4, which shows the Raman spectra of some TiO_2 R+A mixtures ($M_{\text{Rut}} = 24.5, 53.4, \text{ and } 69.4\%$) along with their corresponding mathematical fittings. As can be seen, it is clear the appropriateness of the analysis method as well as the scaling of the Rutile-related phonon contribution as the M_{Rut} advances.

Following this approach, and analogous to XRD, the data provided by the analysis of the Raman spectra can be used to estimate the concentration of Rutile phase in the TiO_2 R+A powder mixtures (Figure 5). The %Rut values were obtained by considering either the intensity (Int) or the area (Area) of the *Lorentzian* functions according to:

$$\%Rut(\text{Int}) = \frac{\text{Int}_R}{\text{Int}_R + \text{Int}_A} \quad \text{and} \quad \%Rut(\text{Area}) = \frac{\text{Area}_R}{\text{Area}_R + \text{Area}_A}, \quad (3)$$

in which Int_R and Area_R are the Raman contributions due to Rutile at ~ 448 and 609 cm^{-1} , and Int_A and Area_A the ones due to Anatase at $\sim 395, 518, \text{ and } 639\text{ cm}^{-1}$. According to Fig. 5, the correspondence between the Raman-derived %Rut and M_{Rut} is exceptionally good and, in most of the cases, the agreement is better than 5%. The only exceptions occurring in the $\sim 30\text{--}50\%$ M_{Rut} ($\sim 50\text{--}70\%$ M_{Rut}) range for the %Rut estimated from the area (intensity) ratios of the Raman spectra.

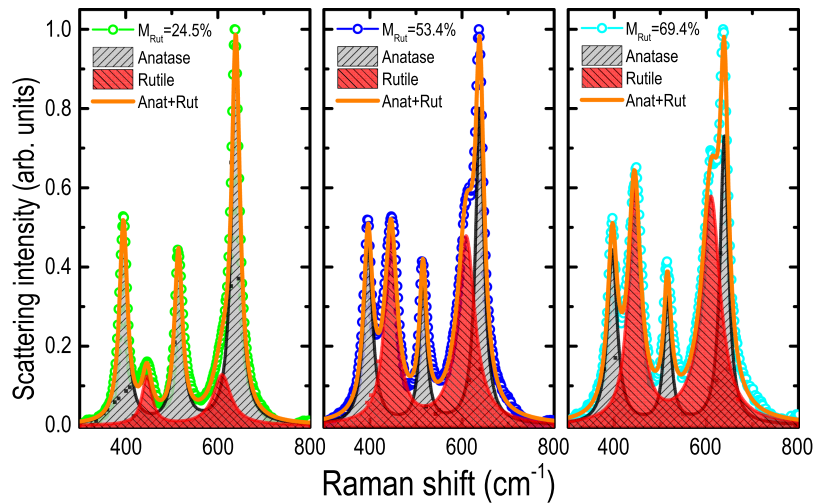


FIG. 4. Deconvolution of Raman spectra into the Rutile and Anatase phases. The experimental Raman spectra were background corrected (straight line removal from $300\text{ to }800\text{ cm}^{-1}$) and fitted with five different *Lorentzian* functions (3Anat + 2Rut). See text for details.

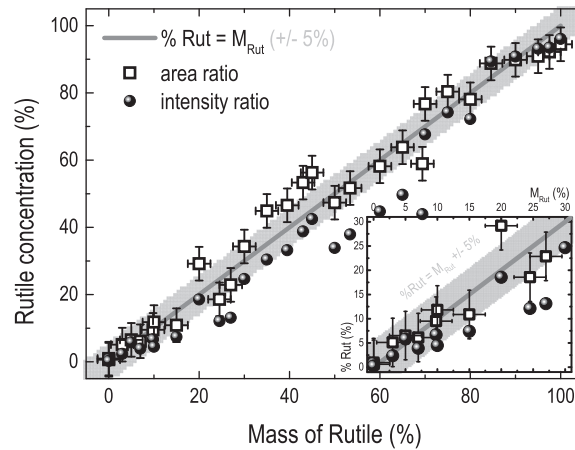


FIG. 5. Concentration of the Rutile crystal phase, as estimated by Raman spectroscopy, as a function of the relative mass of Rutile in TiO_2 R+A powder mixtures. The %Rut values were obtained by combining the intensities or the areas of the *Lorentzian* functions corresponding to the phonon modes due to the Rutile and Anatase phases. The error bars took into account uncertainties in the sample handling ($M_{\text{Rut}} \pm 2.5\%$) and data dispersion involving different Raman scans and fitting results ($\% \text{Rut} \pm 5\%$). For clarity reasons, no error bars were indicated in the %Rut data calculated from the intensity ratio. A straight line denoting the linear relationship between the Rutile concentration and the mass of Rutile ($\% \text{Rut} = M_{\text{Rut}}$), and the region in which $\% \text{Rut} = M_{\text{Rut}} \pm 5\%$ are also shown. The inset shows the $0 \leq M_{\text{Rut}} \leq 30\%$ range in detail.

It happened because, whereas the Raman spectra presented considerable changes in the $\sim 30\text{-}70\%$ mass concentration range (see Fig. 4), the Rutile- and Anatase-related intensity and area ratios didn't, rendering %Rut around 50%. In fact, this is consistent with the increased gap between the %Rut values as provided by the *Lorentzian* intensities and areas ratios.²⁹ Based on the results of Fig. 5 the best %Rut estimates were achieved by considering the Rutile-to-Anatase area ratios, such that $\% \text{Rut} = M_{\text{Rut}} \pm 5\%$, except around $M_{\text{Rut}} \sim 40\%$ in which the deviation reaches $\sim 7.5\%$.

According to the above results and discussion it is possible to establish a comparison involving XRD and Raman spectroscopy when applied to the study of TiO_2 . Clearly, both techniques are able to distinguish between the Rutile and Anatase phases of TiO_2 (Figs. 1 and 3), as well as to provide their relative concentration with reasonable accuracy: around 2 and $< 5\%$ with XRD (Fig. 2) and Raman (Fig. 5), respectively. Their main differences, however, stay in terms of: (1) instrumentation – highly adaptable Raman setups (involving optical fibres and diode lasers operating at different wavelengths) in contrast to the severe layout of XRD diffractometers; and (2) spatial resolution – ranging from millimeters down to hundreds of nanometers by simply changing the Raman spectrometer optics, figures that are hardly attained with standard XRD apparatuses.³⁰ Furthermore, Raman spectroscopy is naturally compatible with the analysis of interfaces, surfaces or thin films and, with proper instrumentation it allows the achievement of 2d (or even 3d) maps with high spectral-spatial resolution.²⁵

IV. CONCLUDING REMARKS

Summarizing, TiO_2 is a relatively simple material that find applications in photovoltaics, photocatalysis, pigments, optical coatings, electronic materials, etc. An important characteristic of the TiO_2 -based materials and devices is related to the presence and relative amount of the Rutile and Anatase crystal phases. In spite of its relevance, so far, the qualitative-quantitative analysis of the TiO_2 polymorphs has been performed almost exclusively by X-ray diffraction. Motivated by these facts, this work presented an alternative method, based on Raman scattering spectroscopy, to estimate the amount of Rutile or Anatase phases in TiO_2 materials. Most of all, the method provides accurate phase analyses without the need for standards or laborious experimental calibration procedures. Within the main advantages of the present experimental approach one can mention: (a) it is relatively fast (spectra acquisition and data analysis around 2-3 min); (b) it is based on simple, low-cost and, in certain cases, portable instrumentation allowing its use in *in-situ* (academic or industrial) applications

and; most importantly (c) it is naturally suitable to investigate thin films and systems with very small dimensions (down the μm^2 range, for example, by using a x100 objective lens). Bearing in mind all of these attributes, the method is expected to contribute with the study of new materials and/or devices based, total or partially, on TiO_2 . In special, one can envisage its use to investigate, with high spatial resolution, the effect of different Rutile-to-Anatase TiO_2 amounts (or distributions) in surfaces, interfaces, low-dimension systems, photocatalytic devices, dye-sensitized solar cells, etc.

ACKNOWLEDGMENTS

The author is indebted to Dr M. I. B. Bernardi for fruitful discussions as well as for the TiO_2 mixtures and XRD characterizations. The present work was financially supported by the Brazilian agencies FAPESP and CNPq.

- ¹ A. J. Frank, N. Kopidakis, and J. van de Lagemaat, *Coord. Chem. Reviews* **248**(13-14), 1165–1179 (2004).
- ² Y. Bai, I. M. Seró, F. Angelis, J. Bisquert, and P. Wang, *Chem. Rev.* **114**(19), 10095–10124 (2014).
- ³ L. Wu, D. Buchholtz, D. Bresser, L. G. Chagas, and S. Passerini, *J. Power Sources* **251**, 379–385 (2014).
- ⁴ A. Fujishima, X. Zhang, and D. A. Tryk, *Surf. Sc. Rep.* **63**, 515–582 (2008).
- ⁵ F. Han, V. S. R. Kambala, M. Srinivasan, D. Rajarathnam, and R. Naidu, *Appl. Catal. A: Gen.* **359**, 25–40 (2009).
- ⁶ T. Rajh, N. M. Dimitrijevic, M. Bissonnette, T. Koritarov, and V. Konda, *Chem. Rev.* **114**(19), 10177–10213 (2014).
- ⁷ H. A. Macleod, in *Thin-film optical filters*, Institute of Physics Publishing (Bristol, 2001), pp. 158.
- ⁸ J. Bai and B. Zhou, *Chem. Rev.* **114**(19), 10131–10176 (2014).
- ⁹ See, for example, J. Nowotny, in *Oxide semiconductors for solar energy conversion - Titanium dioxide* (CRC Press, Boca Raton, 2012), pp. 145.
- ¹⁰ A. D. Paola, M. Bellardita, and L. Palmisano, *Catalysis* **3**, 36–73 (2013).
- ¹¹ D. A. H. Hanaor and C. C. Sorrell, *J. Mater. Sci.* **46**, 855–874 (2011).
- ¹² M. Landmann, E. Rauls, and W. G. Schmidt, *J. Phys.: Condens. Matter* **24**, 195503-1–195503-6 (2012), and references therein.
- ¹³ A. Hagfeldt, G. Boschloo, L. Sun, L. Kloo, and H. Pettersson, *Chem. Rev.* **110**, 6595–6663 (2010).
- ¹⁴ A. Veres, J. Menesi, C. Janaky, G. F. Samu, M. K. Scheyer, Q. Xu, F. Salahioglu, M. V. Garland, I. Dekany, and Z. Zhong, *RSC Adv.* **5**, 2421–2428 (2015).
- ¹⁵ A. Yella, L. P. Heiniger, P. Gao, M. K. Nazeeruddin, and M. Grätzel, *Nano Lett.* **14**, 2591–2596 (2014).
- ¹⁶ T. K. Yun, S. S. Park, D. Kim, J. H. Shim, J. Y. Bae, S. Huh, and Y. S. Won, *Dalton Trans.* **41**, 1284–1288 (2012).
- ¹⁷ C. P. Lee, L. Y. Lin, K. W. Tsai, R. Vittal, and K. C. Ho, *J. Power Sources* **196**, 1632–1638 (2011).
- ¹⁸ R. J. Capwell, F. Spagnolo, and M. A. D. Sesa, *Appl. Spectrosc.* **26**(5), 537–539 (1972).
- ¹⁹ J. C. Parker and R. W. Siegel, *Appl. Phys. Lett.* **57**(9), 943–945 (1990).
- ²⁰ R. J. Gonzalez, “Raman, infrared, X-ray, and EELS studies of nanophase titania” (PhD Thesis, Virginia Tech 1996).
- ²¹ I. M. Clegg, N. J. Everall, B. King, H. Melvin, and C. Norton, *Appl. Spectrosc.* **55**(9), 1138–1150 (2001).
- ²² V. H. C. Sánchez, E. Camps, and M. C. López, *Superficies y Vacío* **27**(3), 88–92 (2014).
- ²³ See, for example, *Encyclopedia of materials characterization: surfaces, interfaces, thin films*, C. R. Bundle, C. A. Evans, and S. Wilson (Eds), Elsevier, Boston 1992.
- ²⁴ R. A. Spurr and H. Myers, *Anal. Chem.* **29**(5), 760–762 (1957).
- ²⁵ *Handbook of Raman Spectroscopy*, I. R. Lewis and H. G. M. Edwards (Eds), Taylor and Francis, NY 2001.
- ²⁶ S. P. S. Porto, P. A. Fleury, and T. C. Damen, *Phys. Rev.* **154**(2), 522–526 (1967).
- ²⁷ T. Oshaka, F. Izumi, and Y. Fujiki, *J. Raman Spectrosc.* **7**(6), 321–324 (1978).
- ²⁸ <http://www.originlab.com/>.
- ²⁹ As expected (and as it was experimentally observed), only the intensities and the areas of the Rutile- and Anatase-related Raman individual contributions changed with MRut, whereas their corresponding line-widths remained essentially the same. As a consequence, since in a *Lorentzian* function the “Area/Int” ratio is proportional to the line-width, the “Area/Int” ratio varies in order to keep the line-width constant.
- ³⁰ M. Hanke, M. Dubschlaff, M. Schmidbauer, T. Boeck, S. Schöder, M. Burghammer, C. Riekel, J. Patommel, and C. G. Schroer, *Appl. Phys. Lett.* **92**, 193109-1–193109-3 (2008).